

X-ray reflection from a curved multilayer mirror

© V.I. Punegov

Physico-Mathematical Institute, Komi Scientific Center, Ural Branch of the Russian Academy of Sciences, Syktyvkar, Russia
E-mail: vpunegov@dm.komisc.ru

Received April 25, 2023

Revised May 22, 2023

Accepted May 22, 2023

A new theoretical method has been developed for calculating the X-ray reflection from a curved multilayer mirror. It is performed the numerical simulation of reciprocal space maps from such mirror, as well as reflection curves in the specular and non-specular directions.

Keywords: curved multilayer X-ray mirror, reciprocal space mapping, two-dimensional recurrence relations.

DOI: 10.61011/TPL.2023.07.56452.19605

X-ray reciprocal space mapping (RSM) is commonly used to examine defects [1] and nanostructures [2] in crystals. In multilayer systems, RSM was performed with the use of hard X-ray [3] and extreme ultraviolet radiation [4] to obtain data on interlayer roughness. Numerical calculation techniques were developed exclusively for diffuse scattering off both crystals and multilayer structures. Coherent scattering, which is significantly more intense than the diffuse component, was either neglected [1,3,4] or taken into account in the form of the instrumental function [2]. Computational techniques for reciprocal space mapping of coherent scattering intensity utilizing two-dimensional recurrence relations (TDRRs) [5,6] and the Takagi–Taupin equations [7] are available at present. It has recently been demonstrated that TDRRs and the Takagi–Taupin equations are identical in the case of dynamical X-ray diffraction in a perfect crystal and transform into each other in passing from a discrete-layered structure to a model of a periodic medium with a continuous electron density [8]. It was also established that numerical calculations based on TDRRs are always stable, whereas calculations utilizing the Takagi–Taupin equations yield unstable solutions in certain cases.

In contrast to planar aperiodic multilayer systems [9], curved multilayer X-ray mirrors (MXRMs) with various surface curvatures belong to the class of lateral gradient structures [10]. Note that elastic bending of crystals may be induced mechanically, while MXRMs are fabricated by depositing multilayer coatings onto substrates with a curved surface profile. Magnetron sputtering is normally used for the purpose. Just as the common one-dimensional recurrence relations of Parratt [11], the two-dimensional recurrence relations obtained earlier are applicable only to planar periodic structures [5,6] and are not suitable for calculations of reflection off curved MXRMs.

In the present study, wave optics and TDRRs are used to formulate a new approach to calculation of X-ray diffraction by curved multilayer mirrors. The two-dimensional recurrence relations from [5,6] are generalized

for this purpose to the case of deformed periodic structures. Modified TDRRs are used to develop an algorithm for calculation of RSMs and their cross sections in vertical (specular) and lateral (non-specular) directions as functions of the MXRM curvature radius. Almost all studies into X-ray reflection off curved MXRMs are concerned with radiation focusing. The present study is, in contrast, focused on the development of a new theoretical approach to nondestructive X-ray diffraction diagnostics of curved multilayer structures.

Two-dimensional recurrence relations have been derived for the first time in order to characterize dynamical X-ray diffraction in a lateral crystal with a rectangular cross section [5]. These relations for transmitted T and diffracted S waves in a perfect planar periodic structure take the form

$$\begin{aligned} T_{n+1}^{m+1} &= (aT_n^m + b_1S_n^m) \exp(i\varphi), \\ S_{n-1}^{m+1} &= (aS_n^m + b_2T_n^m) \exp(i\varphi), \end{aligned} \quad (1)$$

where

$$a = 1 - iq_0, \quad b_1 = -i\bar{q}, \quad b_2 = -iq, \quad q_0 = -\pi\chi_0 d / (\lambda\gamma_0),$$

$$q = C\pi\chi_1 d / (\lambda\gamma_0), \quad \bar{q} = C\pi\chi_{\bar{1}} d / (\lambda\gamma_0),$$

d is the structure period, λ is the X-ray radiation wavelength, C is the X-ray polarization factor, $\gamma_0 = \sin\theta_B$, and θ_B is the Bragg angle. Coefficient $\varphi = \frac{2\pi d}{\lambda \sin\theta_B}$ in TDRRs characterizes the phase difference accumulated in propagation of an X-ray beam within a periodic structure from one numerical calculation grid node to the other.

In a multilayer structure with a double-layer period, Fourier coefficients of X-ray polarizability for a transmitted wave χ_0 , a diffraction wave χ_1 , and a diffraction wave in the transmission direction $\chi_{\bar{1}}$ are written as

$$\begin{aligned} \chi_0 &= \frac{\chi_t d_t + \chi_b d_b}{d}, & \chi_1 &= \frac{\chi_t - \chi_b}{\pi} \sin\left(\pi \frac{d_t}{d}\right), \\ \chi_{\bar{1}} &= \frac{\chi_t - \chi_b}{\pi} \sin\left(\pi \frac{d_b}{d}\right), \end{aligned}$$

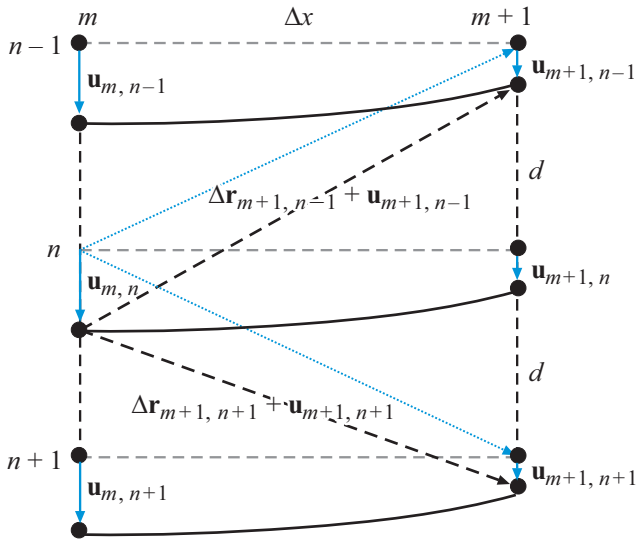


Figure 1. Schematic diagram of nodes of a curved MXRM. The mesh region corresponding to a planar multilayer structure with period d is outlined with dashed lines. Dotted arrows represent vectors $\Delta\mathbf{r}_{m+1, n+1}$ (transmitted wave direction) and $\Delta\mathbf{r}_{m+1, n-1}$ (diffraction wave direction) for a planar multilayer structure. Dashed arrows denote the directions of transmitted and diffraction waves in a curved MXRM.

where $\chi_{t,b}$ and $d_{t,b}$ are the Fourier coefficients of polarizabilities and thicknesses of the top (t) and bottom (b) layers of the structure period.

TDRRs (1) are written in a rectangular coordinate frame with axis x aligned with the entrance surface of a planar MXRM and axis z is directed toward the bulk of the structure. In a two-dimensional periodic grid, axis z is divided into equal sections d that correspond to the period of a planar MXRM (Fig. 1). Sections are numbered from top to bottom as $1, 2, \dots, n, \dots, N_z$, where N_z corresponds to the position of a period at the lower boundary of a multilayer structure and n specifies the node number in the vertical direction. Axis x is then divided into sections $\Delta x = d \cot \theta_B$, where θ_B is the Bragg angle for an incident X-ray beam. The positions of these sections are numbered as $1, 2, \dots, m, \dots, M_x$, where m is the node number in the horizontal direction and M_x is the number of nodes in this direction.

In the general case, nodes (m, n) shift in horizontal and vertical directions in passing from a planar periodic system to a deformed structure. Let nodes with coordinates (m, n) and $(m + 1, n + 1)$ be specified by vectors $\mathbf{r}_{m, n}$ and $\mathbf{r}_{m+1, n+1}$, respectively, in a planar MXRM. Vector $\Delta\mathbf{r}_{m+1, n+1}$ between these nodes in the direction of a transmitted X-ray wave is then written as $\Delta\mathbf{r}_{m+1, n+1} = \mathbf{r}_{m+1, n+1} - \mathbf{r}_{m, n}$ (Fig. 1). Vector $\Delta\mathbf{r}_{m+1, n-1}$ from node (m, n) in the direction of diffraction wave node $(m + 1, n - 1)$ is written accordingly as $\Delta\mathbf{r}_{m+1, n-1} = \mathbf{r}_{m+1, n-1} - \mathbf{r}_{m, n}$. Nodes shift in a deformed periodic structure by, e.g., vector $\mathbf{u}_{m, n}$ for (m, n) . The node

positions then change in the following way:

$$\mathbf{r}_{m, n} \rightarrow \mathbf{r}_{m, n} + \mathbf{u}_{m, n}, \quad \mathbf{r}_{m+1, n+1} \rightarrow \mathbf{r}_{m+1, n+1} + \mathbf{u}_{m+1, n+1}$$

and

$$\mathbf{r}_{m+1, n-1} \rightarrow \mathbf{r}_{m+1, n-1} + \mathbf{u}_{m+1, n-1}.$$

Therefore, the phase factors in TDRRs (1) also change:

$$\begin{aligned} T_{n+1}^{m+1} &= (aT_n^m + b_1S_n^m) \exp(i\varphi_0), \\ S_{n-1}^{m+1} &= (aS_n^m + b_2T_n^m) \exp(i\varphi_1), \end{aligned} \quad (2)$$

where

$$\begin{aligned} \varphi_0 &= \mathbf{k}_0 \Delta\mathbf{r}_{m+1, n+1} + \mathbf{k}_0(\mathbf{u}_{m+1, n+1} - \mathbf{u}_{m, n}) \\ &= \varphi + \mathbf{k}_0(\mathbf{u}_{m+1, n+1} - \mathbf{u}_{m, n}), \\ \varphi_1 &= \varphi + \mathbf{k}_1(\mathbf{u}_{m+1, n-1} - \mathbf{u}_{m, n}), \end{aligned}$$

and $\mathbf{k}_{0,1}$ are the wave vectors of incident and reflected X-ray waves. TDRRs (2) characterize diffraction reflection off a multilayer structure with an arbitrary spatial period variation. Let us consider for simplicity a cylindrically curved MXRM with (m, n) node displacement

$$\mathbf{u}_{m, n} = \mathbf{u}_{m, n} \mathbf{n} = -(\Delta x m)^2 / (2R), \quad (3)$$

where \mathbf{n} is the normal to the surface of a planar periodic structure and R is the curvature radius of a cylindrically curved MXRM. Figure 1 presents the displacement vectors of nodes of a cylindrically curved MXRM, which are directed downward along axis z . The displacement magnitude within a specific column of nodes (e.g., with number m) remains the same for each number n in the vertical direction.

Numerical modeling of RSM was performed using the example of reflection of X-ray radiation (with a photon energy of 2.5 keV and a wavelength of $\lambda = 0.5$ nm) off a

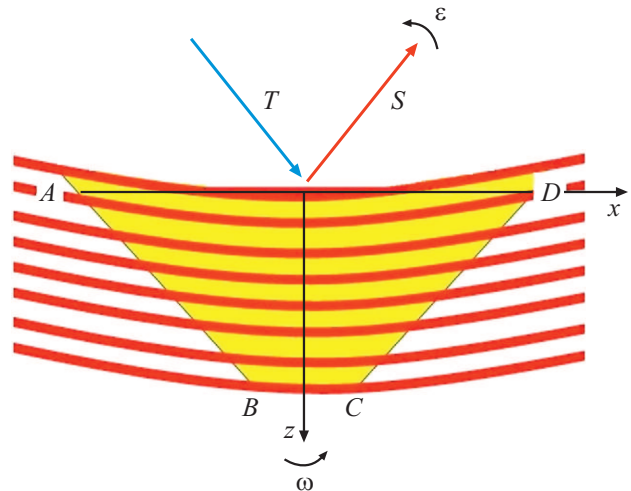


Figure 2. Schematic diagram of X-ray diffraction by a curved MXRM. T — incident beam amplitude, S — reflected (diffracted) beam amplitude, ω — rotation angle of a curved MXRM, and ε — rotation angle of an analyzer.

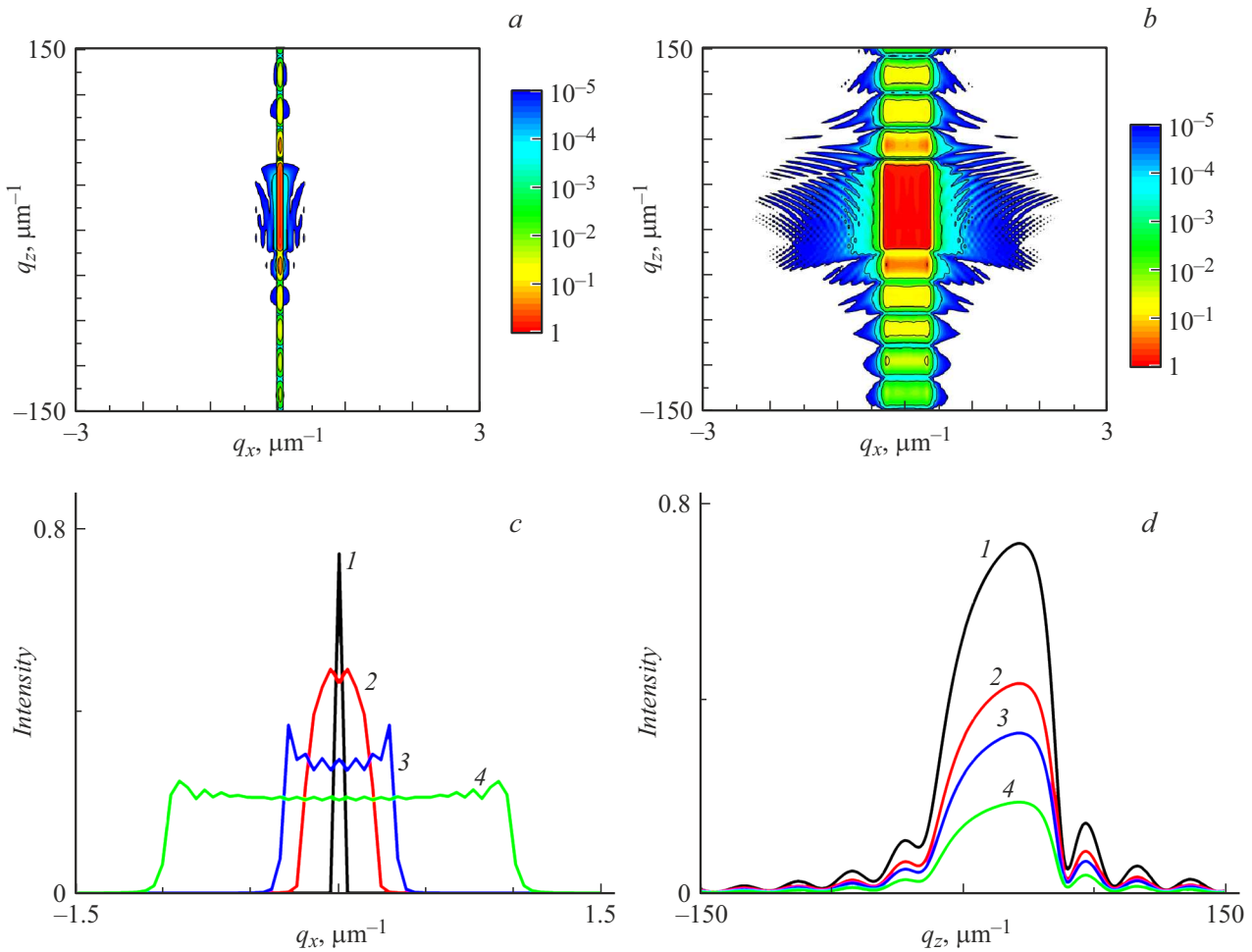


Figure 3. Calculated RSMs for a Pd/B₄C MXRM (*a* — planar multilayer structure; *b* — curved MXRM with a curvature radius of 3 m). *c, d* — Reflection curves for a Pd/B₄C MXRM in lateral (non-specular) and vertical (specular) directions, respectively. *1* — Planar multilayer structure, *2* — curvature radius $R = 5$ m, *3* — $R = 3$ m, and *4* — $R = 1$ m. The lateral width of incident X-ray radiation is $80 \mu\text{m}$.

curved Pd/B₄C MXRM with layer thicknesses $d_{\text{Pd}} = 2$ nm and $d_{\text{B}_4\text{C}} = 2$ nm [12] and varying curvature radii.

A substrate with a curved surface profile may be either amorphous (glass) or single-crystalline (silicon). X-ray radiation is not reflected off an amorphous medium. The lattice period of a single-crystalline substrate is normally an order of magnitude lower than the one-dimensional MXRM period. Since the Bragg condition is unlikely to be fulfilled in both structures with significantly different periods, it is fair to assume that X-ray radiation is also not reflected off a single-crystalline substrate. Thus, the influence of the substrate was neglected in numerical calculations.

The Bragg angle for a multilayer X-ray mirror with period $d = 4$ nm is 3.6° . The Fourier coefficients of polarizabilities of MXRM layers are

$$\chi_{\text{Pd}} = (-0.58 + i0.05) \cdot 10^{-3},$$

$$\chi_{\text{B}_4\text{C}} = (-0.16 + i0.001) \cdot 10^{-3}.$$

The MXRM has 50 periods and a thickness of $0.2 \mu\text{m}$. The primary extinction depth for a multilayer Pd/B₄C structure is $0.073 \mu\text{m}$.

Figure 2 presents the diagram of calculations for mapping the intensity of reflection off a curved MXRM as applied to triple-axis diffractometry. Angles of rotation of a sample (curved MXRM) ω and an analyzer ε are related to projections q_x and q_z of vector $\mathbf{q} = \mathbf{Q} - (2\pi/d)\mathbf{n}$ in the following way:

$$q_x = (2\pi/\lambda) \sin \theta_B (2\omega - \varepsilon),$$

$$q_z = -(2\pi/\lambda) \cos \theta_B \varepsilon,$$

where $\mathbf{Q} = \mathbf{k}_1 - \mathbf{k}_0$ is the diffraction vector.

The MXRM surface region irradiated by an incident X-ray beam (length AD in Fig. 2) with a lateral width of $80 \mu\text{m}$ is $L_x = \Delta x d = 1.3$ mm. If the sizes of incident and diffracted beams are the same, the diffraction X-ray field of a spatially limited wave in a curved multilayer mirror forms primarily within trapezoid $ABCD$ [8]. The procedure for calculation of RSMs with TDRRs was detailed in [5,8].

Figure 3 shows the calculated RSMs for planar and curved (with a curvature radius of $R = 3$ m) Pd/B₄C MXRMs. Equal-intensity contours are plotted on a logarithmic scale; the coefficient of reflection off a planar multilayer structure is 0.7. The angular distribution of diffracted intensity for the curved MXRM is normalized by multiplication by a factor of 50. Figures 3, *c* and *d* present the reflection curves for the Pd/B₄C MXRM in lateral (non-specular) and vertical (specular) directions, respectively. As the curvature radius decreases (lateral deformation intensifies), q_x cross sections of RSMs broaden (Fig. 3, *c*). The profiles of q_z cross sections of maps do not vary in shape, since the MXRM period remains unchanged. Note that the profile of the q_z cross section of the Pd/B₄C planar multilayer structure matches the reflection curve from [11].

In the present study, the procedure of calculation of the angular distribution of coherent scattering intensity in reciprocal space was demonstrated using the example model of a cylindrically curved multilayer X-ray mirror. RSMs for MXRMs have been obtained earlier with the use of hard [3] and soft [4] X-ray radiation to examine the specifics of diffuse scattering off interlayer roughness. The more intense coherent component was neglected in numerical calculations [3,4], which made it somewhat more difficult to retrieve data on the structural characteristics of multilayer systems. One may obtain more accurate information regarding the MXRM structure by calculating the total scattering intensity with coherent and diffuse components.

The developed approach is also applicable in the analysis of X-ray reflection off MXRMs with other curvature geometries (specifically, elliptical [10], parabolic [13], and hyperbolic [14] curvature). Matrix elements of node displacement $u_{m,n}$ for such multilayer structures change in both lateral and vertical directions in accordance with the MXRM curvature profile.

Funding

This study was supported by a grant from the Russian Science Foundation, project № 23-22-00062 (<https://rscf.ru/project/23-22-00062/>).

Conflict of interest

The author declares that he has no conflict of interest.

References

- [1] P.F. Fewster, N.L. Andrew, *J. Phys. D: Appl. Phys.*, **28**, A97 (1995). DOI: 10.1088/0022-3727/28/4A/019
- [2] V.I. Punegov, *Phys.-Usp.*, **58** (5), 419 (2015). DOI: 10.3367/UFNr.0185.201505a.0449 [V.I. Punegov, *Phys. Usp.*, **58**, 419 (2015). DOI: 10.3367/UFNe.0185.201505a.0449].
- [3] E. Majkova, Y. Chushkin, M. Jergel, S. Luby, V. Holy, I. Matko, B. Chenevier, L. Toth, T. Hatano, M. Yamamoto, *Thin Solid Films*, **497**, 115 (2006). DOI: 10.1016/j.tsf.2005.10.051
- [4] A. Haase, V. Soltwisch, S. Braun, C. Laubis, F. Scholze, *Opt. Express*, **25**, 15441 (2017). DOI: 10.1364/OE.25.015441
- [5] V.I. Punegov, S.I. Kolosov, K.M. Pavlov, *Acta Cryst. A*, **70**, 64 (2014). DOI: 10.1107/S2053273313030416
- [6] V.I. Punegov, S.I. Kolosov, K.M. Pavlov, *J. Appl. Cryst.*, **49**, 1190 (2016). DOI: 10.1107/S1600576716008396
- [7] V.I. Punegov, K.M. Pavlov, A.V. Karpov, N.N. Faleev, *J. Appl. Cryst.*, **50**, 1256 (2017). DOI: 10.1107/S1600576717010123
- [8] V.I. Punegov, S.I. Kolosov, *J. Appl. Cryst.*, **55**, 320 (2022). DOI: 10.1107/S1600576722001686
- [9] C. Morawe, E. Ziegler, J.-C. Peffen, I.V. Kozhevnikov, *Nucl. Instrum. Meth. Phys. Res. A*, **493**, 189 (2002). DOI: 10.1016/S0168-9002(02)01570-X
- [10] H. Mimura, T. Kimura, H. Yumoto, H. Yokoyama, H. Nakamori, S. Matsuyama, K. Tamasaku, Y. Nishino, M. Yabashi, T. Ishikawa, K. Yamauchi, *Nucl. Instrum. Meth. Phys. Res. A*, **635**, S16 (2011). DOI: 10.1016/j.nima.2010.11.047
- [11] L.G. Parratt, *Phys. Rev.*, **95**, 359 (1954). DOI: 10.1103/PhysRev.95.359
- [12] N. An, X. Du, Q. Wang, Z. Cao, S. Jiang, Y. Ding, *Proc. SPIE*, **9211**, 92110I (2014). DOI: 10.1117/12.2060772
- [13] M. Schuster, H. Gobel, *J. Phys. D: Appl. Phys.*, **28**, A270 (1995). DOI: 10.1088/0022-3727/28/4A/053
- [14] S. Matsuyama, J. Yamada, K. Hata, Y. Kohmura, M. Yabashi, T. Ishikawa, K. Yamauchi, *Microsc. Microanal.*, **24**, 284 (2018). DOI: 10.1017/S1431927618013764

Translated by D.Safin